UNIVERSITY
OF TRENTO

DEPARTMENT OF INFORMATION AND COMMUNICATION TECHNOLOGY

38050 Povo – Trento (Italy), Via Sommarive 14
http://www.dit.unitn.it

LOCATION AND IMAGING OF TWO-DIMENSIONAL SCATTERERS BY USING A PARTICLE SWARM ALGORITHM

Salvatore Caorsi, Massimo Donelli, Andrea Lommi, and Andrea Massa

August 2004

Technical Report DIT-04-072

Location and Imaging of Two-Dimensional Scatterers by using a Particle Swarm Algorithm

Salvatore Caorsi*, Massimo Donelli**, Andrea Lommi**, and Andrea Massa**

*Department of Electronics

University of Pavia, Via Ferrata 1, 27100 Pavia - Italy

Tel. +39 0382 505661, Fax +39 0382 422583

**Department of Information and Communication Technology

University of Trento, Via Sommarive 14, 38050 Trento - Italy

Tel. +39 0461 882057, Fax +39 0461 882093, E-mail: *andrea.massa@ing.unitn.it, massimo.donelli@dit.unitn.it*

Corresponding Author:

Andrea MASSA

Department of Information and Communication Technology

University of Trento, Via Sommarive 14, 38050 Trento - Italy

Tel. +39 0461 882057, Fax +39 0461 882093, E-mail: *andrea.massa@ing.unitn.it*

Location and Imaging of Two-Dimensional Scatterers by using a Particle Swarm Algorithm

Salvatore Caorsi*, Massimo Donelli**, Andrea Lommi**, and Andrea Massa**

Abstract

In this paper, a microwave imaging method for reconstructing two-dimensional dielectric scatterers is presented. Staring from an integral formulation of the electromagnetic scattering phenomena, the method is aimed at determining the dielectric profile of the scatterer under test by means of an innovative particle swarm algorithm. In order to preliminary assess the effectiveness of the proposed method, some numerical experiments are carried out in noiseless as well as in noisy conditions. The obtained results confirm the capabilities of the proposed method in term of reconstruction accuracy and robustness.

Key words:

Microwave Imaging, Inverse Scattering, Particle Swarm Algorithm

1 Introduction

Tomographic microwave imaging techniques are aimed at producing a two-dimensional map of the electromagnetic properties of a region of interest (namely the *investigation domain*) from measurements of the field taken outside that region [1]. The object image can prove very useful in medical diagnosis [2], non-destructive evaluation [3], and sub-surface monitoring [4]. Unfortunately, the determination of medium properties requires inverting Lippmann-Schwinger equations [5] and consequently, the solution of an ill-posed and nonlinear problem. Generally, a regularized solution is defined as the global minimum of a suitable cost function [6].

Due to the nonlinear nature of the arising cost function, deterministic procedures will converge to the sought result when started within a proper sphere of the solution space enclosing the solution [7]. Unfortunately, it results very difficult to evaluate the extent of the global minimum attraction basin so that the reliability of the approach cannot be guaranteed and the trial solution could be trapped in a local minimum.

In order to overcome this drawback, global optimization approaches have been successfully applied (see [8][9][10] and the references therein) but, because of the computational cost proportional to the dimension of the problem at hand, practicable serial single-step implementations are limited to a relatively small resolution accuracy and parallel implementations are currently under test [11]. On the other hand, a large number of control parameters need to be set. Consequently, a time-consuming heuristic tuning is required or generally sub-optimal values should be considered [12].

Recently, an innovative evolutionary technique called *Particle Swarm Optimization* (PSO) have been proposed in order to accomplish the same goal of other global optimization methods in a new and faster way [15]. Compared to GA, the main advantage of PSO lies in the minor complexity of the algorithm especially in the tuning phase due to the few control parameters to be calibrated. PSO have been successfully applied in many engineering areas as artificial neural network training [16], fuzzy system control [17],

biomedical applications [18], and power-system stabilizers design [19]. Then, the purpose of this paper is to investigate the foundations and the performances of the PSO algorithm when applied to the microwave imaging problem.

The paper is organized as follows. Section 2 is aimed at describing the microwave imaging problem. In Section 3, the PSO algorithm is presented and customized to the inverse scattering problem. Successively (Section 4), some numerical experiments are reported in order to preliminary assess the capabilities of the PSO algorithm in dealing with highly nonlinear inverse scattering problems. Finally (Section 5), some conclusions point out current limitations and also future developments of the proposed methodology.

2 Mathematical Formulation

Let us consider the two-dimensional scenario shown in Figure 1 where an unknown scatterer, characterized by the following object function

$$\tau(x,y) = \epsilon_r(x,y) - 1 - j\frac{\sigma(x,y)}{2\pi f} \quad (x,y) \in S \tag{1}$$

where ϵ_r and σ are the relative permittivity and conductivity, respectively, lies in an investigation domain, D, illuminated by a set of V incident electromagnetic fields of TM type, $E^{\upsilon}_{inc}(x,y)\ \upsilon = 1, ..., V$, radiated by an electromagnetic source operating at the working frequency f. The background medium is assumed to be lossless, non-magnetic, homogeneous and characterized by known dielectric parameters, $\tau(x,y) = \tau_0\ (x,y) \in \{D - S\}$.

Starting from the measure of the scattered electric field, $E^{\upsilon}_{scatt}(x_p, y_p)\ \upsilon = 1, ..., V;\ p = 1, ..., P$, collected in a set of P measurement points lying in the observation domain, O, and from the knowledge of the incident electric field, $E^{\upsilon}_{inc}(x,y)\ \upsilon = 1, ..., V$, inside the investigation domain, the problem is recast in an optimization one by defining the

following discretized (according to the Richmond's formulation [20]) cost function:

$$\Phi\left\{\underline{f}\right\} = \left\{\frac{\sum_{v=1}^{V}\sum_{p=1}^{P}\left|E_{scatt}^{v}(x_p,y_p)-\zeta_{scatt}^{v}\left\{\underline{f}(x_p,y_p)\right\}\right|^2}{\sum_{p=1}^{P}\sum_{v=1}^{V}\left|E_{scatt}^{v}(x_p,y_p)\right|^2}\right\} + \alpha\left\{\frac{\sum_{v=1}^{V}\sum_{n=1}^{N}\left|E_{inc}^{v}(x_n,y_n)-\xi_{inc}^{v}\left\{\underline{f}(x_n,y_n)\right\}\right|^2}{\sum_{v=1}^{V}\sum_{n=1}^{N}\left|E_{inc}^{v}(x_n,y_n)\right|^2}\right\} \tag{2}$$

$\underline{f}(x_n, y_n) = \{\tau(x_n, y_n), E_{tot}^{v}(x_n, y_n); n = 1, ..., N; v = 1, ..., V\}$ being the unknown array and where $\zeta_{scatt}^{v}(x, y) = j\frac{k_0^2}{4}\int_D \tau(x', y')E_{tot}^{v}(x', y')G_{2D}\,(x, y \mid x', y')\;dx'dy'\;(x, y) \in O$, $\xi_{inc}^{v}(x, y) = E_{tot}^{v}(x, y) - \zeta_{scatt}^{v}(x, y)\;(x, y) \in D$, G_{2D} is the two-dimensional Green's function of the background medium [5], α is a regularizing constant, and the index n denotes a discretization sub-domain of D.

Due to the nonlinearity of the inverse scattering equations [21], the approach for the minimization of (2) should be able to avoid (by recurring to a global optimization technique [8][10]) or to limit (by considering a suitable choice of the searched unknown [22][23]) the occurrence of local minima. In the framework of multiple-agent global optimization techniques, the particle swarm algorithm (PSO) [24] represents an innovative and very promising technique [25].

3 Particle swarm algorithm

The PSO is a stochastic multiple-agent algorithm for finding optimal regions of complex search spaces through the interaction of individuals in a population of particles. The algorithm is based on a metaphor of social interactions and simulates the collective behavior of simple individuals interacting with their environment and each other. In the same way of other population based optimization approaches [26], PSO updates the set of individuals according to the cost function (or *fitness function*, Φ) information so that the population move towards better solution areas. Instead of using evolutionary operators to manipulate the individuals, each individual (called *particle*, $\underline{f} = \{f_i;\ i = 1, ..., I\}$ being $I = (N + 1) \times V$) flies as a "bird" in the search space with a velocity dynamically changed

according to its experience and the experience of other particles.

The PSO, when applied in the framework of microwave imaging to minimize (2), requires the definition of a population of particles (or *particle swarm*)

$$S_0 = \left\{ \underline{f}_0^{(q)};\ q = 1, ..., Q \right\} \tag{3}$$

and a corresponding flying velocity array

$$V_0 = \left\{ \underline{v}_0^{(q)};\ q = 1, ..., Q \right\} \tag{4}$$

Q being the dimension of the trial solution population. Iteratively (being k the iteration number), the trial solutions are ranked according their fitness measures

$$F_k = \left\{ \Phi \left\{ \underline{f}_k^{(q)} \right\};\ q = 1, ..., Q \right\} \tag{5}$$

The best swarm particle ($\underline{f}_k^{(opt)} = arg \left[min_q \left(\Phi \left\{ \underline{f}_k^{(q)} \right\} \right) \right]$) and the best previous position of each particle ($\underline{f}_k^{(\widetilde{q})} = arg \left[min_{h=1,..,k} \left(\Phi \left\{ \underline{f}_h^{(q)} \right\} \right) \right]$) are stored. Then, new swarms of trial solutions are obtained updating each particle according to the following equation

$$f_{i,k+1}^{(q)} = f_{i,k}^{(q)} + v_{i,k+1}^{(q)} \tag{6}$$

being

$$v_{i,k+1}^{(q)} = \omega\, v_{i,k}^{(q)} + \beta \left(f_{i,k}^{(\widetilde{q})} - f_{i,k}^{(q)} \right) + \gamma \left(f_{i,k}^{(opt)} - f_{i,k}^{(q)} \right) \tag{7}$$

where β and γ are two random values included in the range $[0, 2]$ with a uniform distribution generated by a pseudo-random number generator; ω is the *inertia* weight [27].

The iterative process stops when the termination criterion, based on a maximum number of iterations, K (i.e., $k = K$) or on a threshold on the fitness measure, δ (i.e., $\underline{f}_{k*}^{(opt)} \leq \delta$), is verified and $\underline{f}_{k*}^{(opt)}$ is assumed as the microwave imaging problem solution.

4 Numerical Results

In this section, some tomographic reconstructions obtained by using simulated data are presented in order to numerically assess the effectiveness of the PSO-based inverse scattering procedure. In the numerical examples, an object of unknown support S, whose contrast has to be reconstructed, is positioned inside a test square domain, D, of known dimensions $\lambda_0 \times \lambda_0$ (λ_0 being the wavelength of the background medium). The test domain is partitioned into $N = 10 \times 10$ sub-squares. The observation domain is chosen to be a circle of radius λ_0 where $P = 10$ uniformly distributed receivers are located. The investigation domain is illuminated with plane waves incident from a set of known angles $\theta_{inc}^{v} = (v-1)\,\frac{\pi}{2}$; $v = 1, ..., V$; $V = 4$. A multi-illumination/multi-view [5] acquisition system is adopted. The object to be reconstructed consists of a off-centered square cylinder, $\frac{3}{10}\lambda_0 \times \frac{3}{10}\lambda_0$, with dielectric permittivity $\epsilon_r(x, y) = 2.5$ as shown in Fig. $2(a)$.

For the forward problem, in order to avoid the possibility of committing the "inverse crime" (by using the same numerical method in the inversion algorithm as is used for solving the direct problem to produce the synthetic measured data), a different discretization of the investigation domain has been taken into account ($N_{FP} = 50 \times 50$). Moreover, the initial values of the object function for the iterative procedure have been always assumed equal to the background value, and the starting guess for the field distribution equal to the incident field. As far as the setting parameters for the PSO are concerned, the following values have been chosen: $Q = 200$, $K = 2.0 \times 10^4$, $\delta = 10^{-4}$, and $\omega = 0.4$. The inertia weight parameter controls the balance between the global and local search capabilities of the optimization procedure. Similarly to the temperature parameter in simulated annealing method [8], a large inertia weight facilitates a global search while a small inertia facilitates a local search. According to the literature suggestions and in this preliminary PSO assessment, a value equal to 0.4 seems to guarantee a good trade-off between convergence rate and capability to avoid the solution be trapped in local minima of the cost function. On the other hand, various tests on classical benchmarks confirm

that the PSO with different population size has almost the similar performances [27]. Consequently, the choice of a population dimension equal to 200 seems to be appropriate also if more detailed comparisons are necessary in order to extend general considerations to the microwave imaging framework.

Figure 2 gives reconstructed images of the investigation domain at different iterations of the iterative PSO-based approach. Starting from the empty distribution (Fig. $2(b)$, where the dashed line indicates the reference perimeter of the actual object), when the number of iterations increases, the background becomes more clear and the location as well as the reconstruction of the scatterer more accurate. At the convergence iteration, $k^{opt} = 5200$ (Fig. $2(f)$), the estimated profile results very close to the reference profile (Fig. $2(a)$). Moreover, it should be observed the smooth distribution of the permittivity values inside the scatterer domain as well as a clear identification of the scatterer edges obtained without additional terms in the functional to be minimized aimed at achieving these characteristics.

For comparison purposes, Figure 3 shows the reconstructed profiles obtained by applying inversion procedures based on a standard conjugate-gradient algorithm (Fig. $3(a)$), on a suitable genetic algorithm (GA) (Fig. $3(b)$), and on the PSO-based procedure (Fig. $3(c)$). As far as the GA method is concerned the following parameter configuration has been used: $Q = 200$, $P_c = 0.7$ (crossover probability), $P_m = 0.8$ (mutation probability), $P_{bm} = 0.01$ (bit-mutation probability).

In order to quantitatively evaluate the reconstruction accuracy, let us define the following normalized reconstruction error

$$\chi_j = \frac{1}{N_j} \sum_{i=1}^{N_j} \left\{ \frac{|\tau(x_i, y_i) - \tau_{actual}(x_i, y_i)|}{\tau_{actual}(x_i, y_i)} \right\} \times 100 \tag{8}$$

where τ and τ_{actual} are the values of the reconstructed and actual object function, N_j can range over the whole investigation domain ($j \Longrightarrow tot$), or over the area where the actual scatterer is located ($j \Longrightarrow int$), or over the background belonging to the investigation

domain ($j \implies ext$), has been assumed as quality figure. Table I summarizes the obtained results. As can be observed, the PSO approach slightly outperforms the GA-based method ($\chi_{tot}^{(GA)} = 1.8$ versus $\chi_{tot}^{(PSO)} = 1.7$, and $\chi_{int}^{(GA)} = 9.0$ versus $\chi_{int}^{(PSO)} = 8.9$). But if the GA requires (in its preliminary implementation for microwave imaging applications) the calibration of different probabilities or the definition of customized meta-heuristic strategies, the PSO requires the tuning of only one parameter (i.e., the inertia weight ω).

Finally, to examine the stability of the PSO method, an additive noise has been added to the measured data. Let us consider a gaussian noise characterized by an assigned signal-to-noise ration, SNR. Figure 4 shows the inversion results for a SNR varying between $30\,dB$ to $5\,dB$. As expected, it results that although the computational burden notably increases (e.g., $k^{opt} = 0.7 \times 10^4$ for a $SNR = 30\,dB$ versus $k^{opt} = 1.5 \times 10^4$ in correspondence with $SNR = 20\,dB$) the reconstruction accuracy as well as the decreasing in the cost function strongly reduces as shown in Tab. II. However, also in high-noise conditions ($SNR = 5\,dB$), the location and the shaping of the scatterer are acceptable and limited spatial noise (easily detectable and avoidable with simple additive penalty terms in the cost function) appears in the reconstructed background.

5 Conclusions

An inverse-scattering approach based on the particle swarm algorithm has been presented. The method has been applied to the reconstruction of two dimensional dielectric scatterers placed inside an inaccessible domain. In order to asses the capabilities of the proposed method, some preliminary results have been presented and compared with those obtained with state-of-the-art approaches. Quite satisfactory results have been achieved in noiseless as well as in noisy conditions which seems to candidate the PSO-approach as an useful tool for microwave imaging applications. However, in order to completely determine the effectiveness and limitations of the proposed procedure, future researches are mandatory. In this framework, particular attention should be devoted in defining an accurate trade-

off between local and global searching achievable, for example, by linearly decreasing the inertia weight from its initial value during the iterative process or with an adaptive unsupervised tuning of the same quantity.

References

[1] D. Colton and R. Kress. *Inverse Acoustic and Electromagnetic Scattering Theory.* New York: Springer-Verlag, 1992.

[2] Z. H. Cho, J. P. Jones, and M. Singh. *Foundations of Medical Imaging.* New York: Wiley, 1993.

[3] J. Ch. Bolomey, "Microwave imaging techniques for NDT and NDE," *Proc. Training Workshop on Advanced Microwave NDT/NDE Techniques*, Paris, September 1999, pp. 1-66.

[4] A. J. Devaney, "Geophysical diffraction tomography," *IEEE Trans. Geosci. Remote Sensing*, vol. 22, pp. 3-13, 1984.

[5] S. Caorsi, G. L. Gragnani, and M. Pastorino, "An electromagnetic imaging approach using a multi-illumination technique," *IEEE Trans. Biomedical Eng.*, vol. 41, pp. 406-409, 1994.

[6] R. E. Kleinman and P. M. van den Berg, "A modified gradient method for two-dimensional problems in tomography," *J. Computat. Appl. Math.*, vol. 42, pp. 17-35, 1992.

[7] J. M. Ortega and W. C. Rheinboldt. *Iterative Solutions of Non-linear Equations in Several Variables.* Orlando, FL: Academic, 1987.

[8] L. Garnero, A. Franchois, J.-P. Hugonin, Ch. Pichot, and N. Joachimowicz, "Microwave imaging - Complex permittivity reconstruction by simulated annealing," *IEEE Trans. Microwave Theory Tech.*, vol. 39, pp. 1801-1807, 1991.

[9] Z. Q. Meng, T. Takenaka, and T. Tanaka, "Image reconstruction of two-dimensional impenetrable objects using genetic algorithms," *J. Electromagn. Waves Applicat.*, vol. 13, pp. 95-118, 1999.

[10] S. Caorsi, A. Massa, and M. Pastorino, "A computational technique based on a real-coded genetic algorithm for microwave imaging purposes," *IEEE Trans. Geosci. Remote Sensing*, vol. 38, pp. 1697-1708, 2000.

[11] A. Massa *et al.*, "Parallel implementation of a GA-based approach for microwave imaging applications," submitted to *IEEE Trans. Antennas Propagat.*.

[12] D. H. Wolpert and W. G. Macready, "No free lunch theorems for optimization," *IEEE Trans. Evolutionary Computations*, vol. 1, pp. 67-82, 1997.

[13] A. Abubakar, P. M. van den Berg, and J. Mallorqui, "Imaging of biomedical data using a multiplicative regularized contrast source inversion method," *IEEE Trans. Microwave Theory Tech.*, vol. 50, pp. 1761-1771, 2002.

[14] A. Massa *et al.*, "On the effectiveness of an adaptive regularization strategy for microwave imaging problems," *IEEE Antennas Wireless Propagation Lett.*, (submitted).

[15] J. Kennedy, R. C. Eberhart, and Y. Shi. *Swarm Intelligence*. San Francisco: Morgan Kaufmann Publishers, 2001.

[16] R. Mendes, P. Cortez, M. Rocha, and J. Neves, "Particle swarms for feedforward neural network training," *Proc. 2002 Int. Joint Conference on Neural Networks* (IJCNN'02), 2002, vol. 2, pp. 1895-1899.

[17] A. Esmin, A. R. Aoki, and G. Lambert-Torres, "Particle swarm optimization for fuzzy membership function optimization," *Proc. 2002 IEEE Int. Conference Systems, Man and Cybernetics*, 2002, vol. 3, pp. 108-113.

[18] R. C. Eberhart and X. Hu, "Human tremor analysis using particle swarm optimization," *Proc. 1999 Congress on Evolutionary Computation* (CEC'99), Washington, DC, 1999, vol. 3, pp. 1930-1932.

[19] M. A. Abido, "Optimal design of power-system stabilizers using particle swarm optimization," *IEEE Trans. Energy Conversion*, vol. 17, pp. 406-413, 2002.

[20] J. H. Richmond, "Scattering by a dielectric cylinder of arbitrary cross section shape," *IEEE Trans. Antennas Propagat.*, vol. 13, pp. 334-341, 1965.

[21] O. M. Bucci, N. Cardace, L. Crocco, and T. Isernia, "Inverse scattering: Evaluation of degree of nonlinearity and a new solution strategy," *Proc. IEEE Antennas Propagat. Symp.*, Salt Lake City, UT, July 2000, pp. 1752-1755.

[22] T. Isernia, V. Pascazio, and R. Pierri, "A nonlinear estimation method in tomographic imaging," *IEEE Trans. Geosci. Remote Sensing*, vol. 35, pp. 910-923, 1997.

[23] S. Caorsi, M. Donelli, D. Franceschini, and A. Massa, "A new methodology based on an iterative multi-scaling for microwave imaging," *IEEE Trans. Microwave Theory Tech.*, April 2003.

[24] J. Kennedy and R. C. Eberhart, "Particle swarm optimization," *Proc. IEEE Int. Conference Neural Networks*, vol. IV, Perth, Australia, November/December 1995, pp. 1942-1948.

[25] J. Kennedy and W. M. Spears, "Matching algorithms to problems: An experimental test of the particle swarm and some genetic algorithms on the multimodal problem generator," *Proc. IEEE Int. Conference Evolutionary Computation*, 1998.

[26] D. E. Goldberg, *Genetic Algorithms in Search, Optimization, and Machine Learning.* Addison-Wesley, Reading, Mass., 1989.

[27] Y. H. Shi and R. C. Eberhart, "Parameter selection in particle swarm optimization," *Proc. 1998 Annual Conference on Evolutionary Programming*, San Diego, 1998.

Figure Caption

- Figure 1. Problem Geometry.
- Figure 2. Iterative Process - Estimated permittivity distributions at the iteration (b) $k = 0$, (c) $k = 1000$, (d) $k = 2000$, (e) $k = 4000$, and (f) $k = k^{opt}$. (a) Reference distribution.
- Figure 3. Reconstruction accuracy - Estimated permittivity distribution with (a) CG-based Procedure, (b) GA-based Procedure, and (c) PSO-based Procedure.
- Figure 4. Noisy Conditions - Estimated permittivity distributions with PSO-based Procedure when (a) $SNR = 30\,dB$, (b) $SNR = 20\,dB$, (c) $SNR = 10\,dB$, and (d) $SNR = 5\,dB$.

Table Caption

- Table I. Noiseless Conditions - Error Figures.
- Table II. Noisy Conditions - Error Figures.

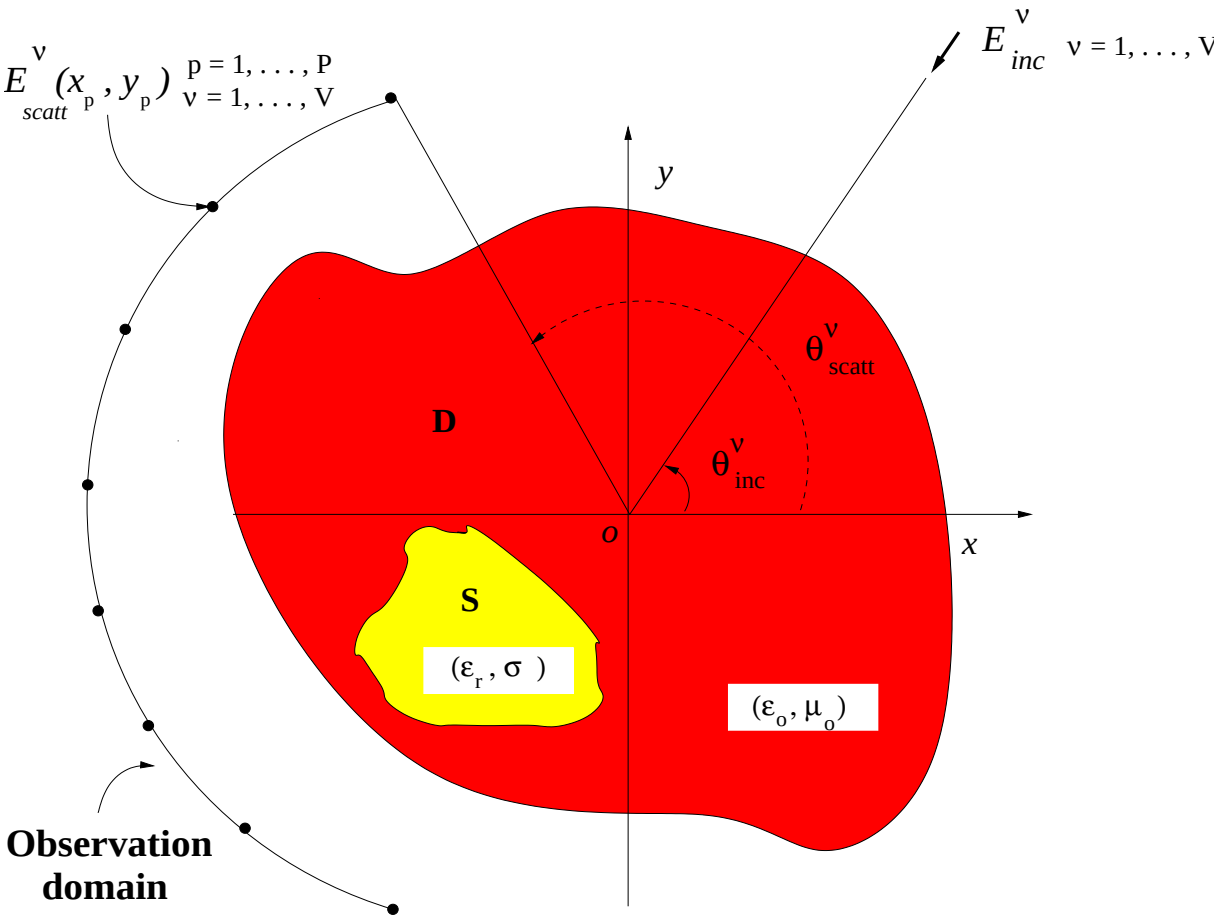

Fig. 1 - S. Caorsi *et al.*, "Location and Imaging of ..."

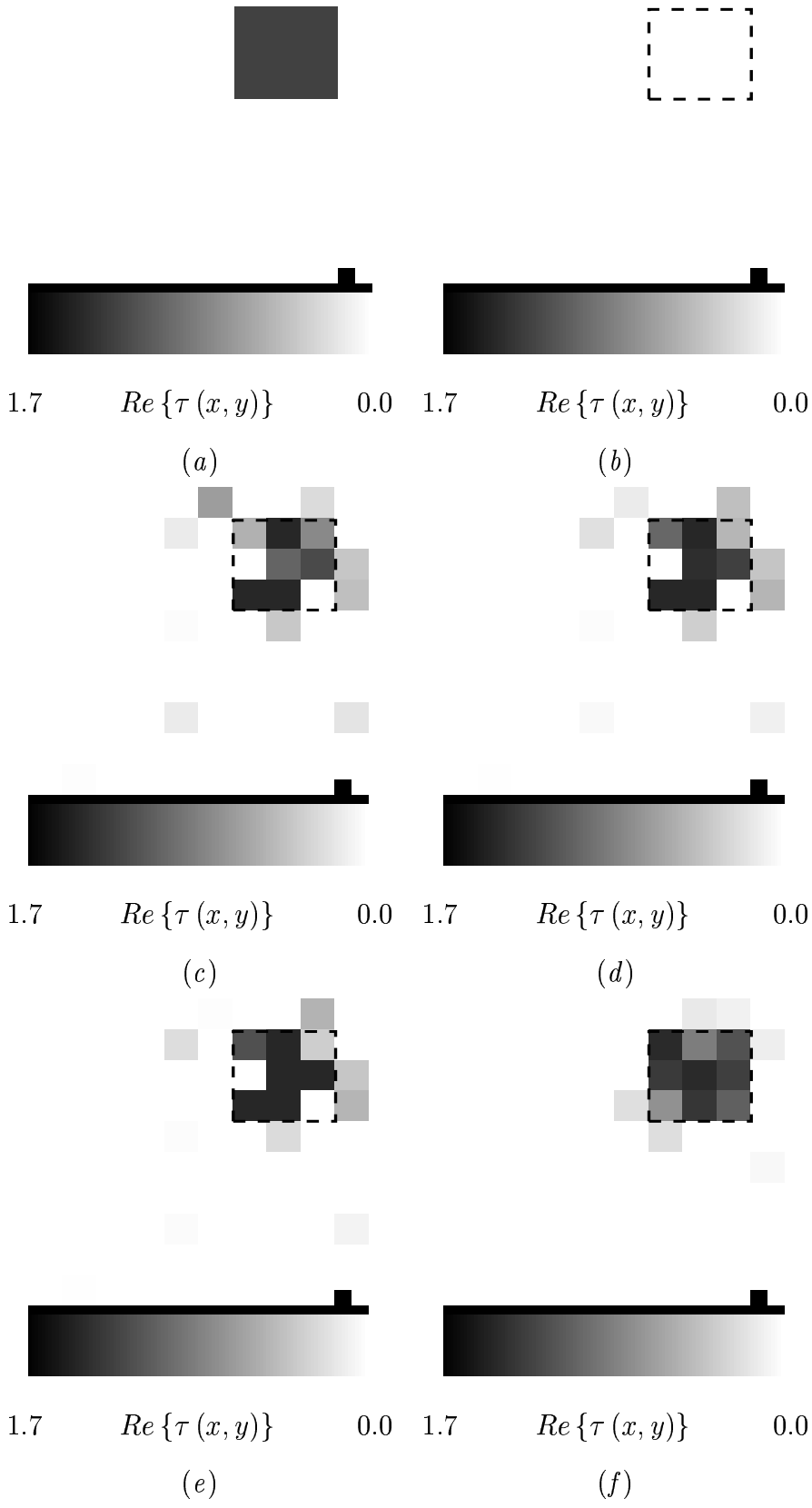

Fig. 2 - S. Caorsi *et al.*, "Location and Imaging of ..."

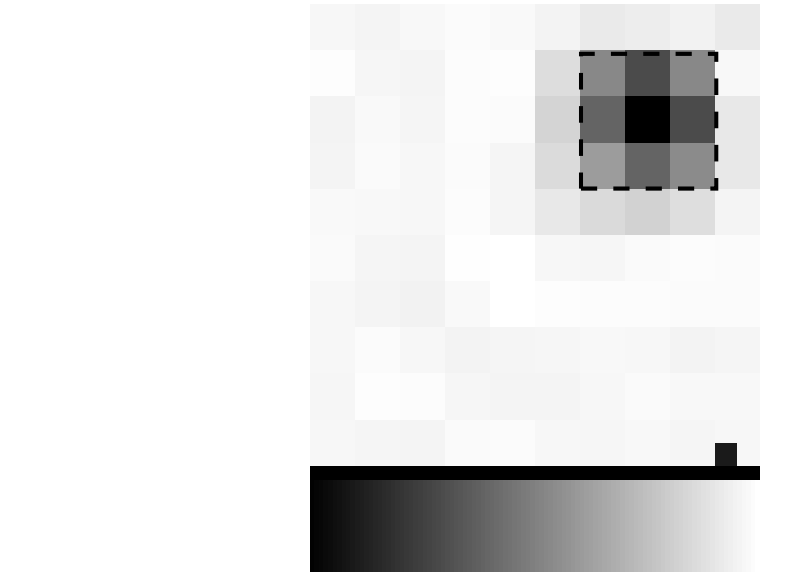

1.7 $Re\{\tau(x,y)\}$ 0.0

(a)

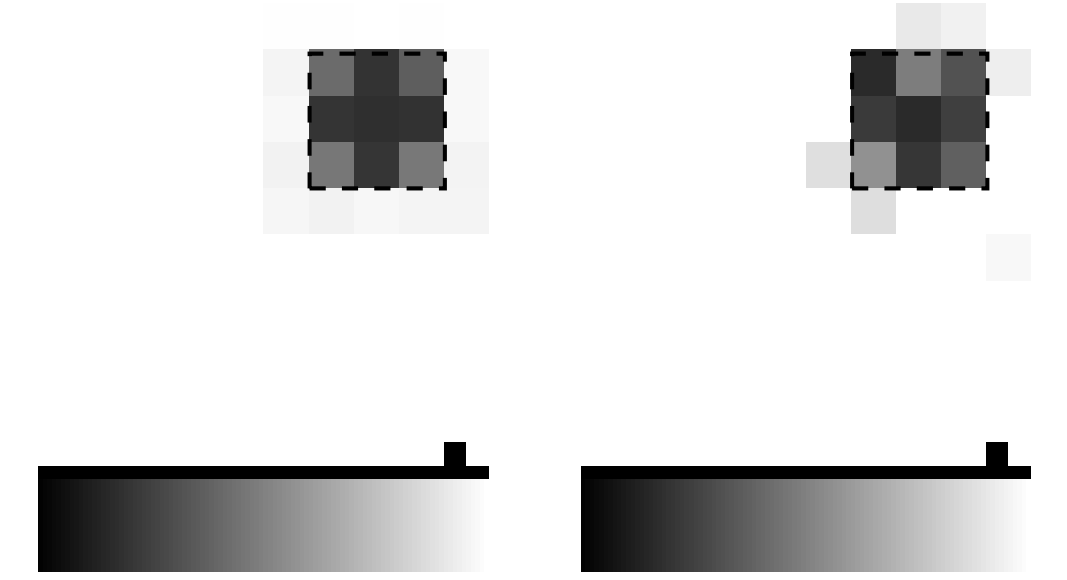

1.7 $Re\{\tau(x,y)\}$ 0.0 1.7 $Re\{\tau(x,y)\}$ 0.0

(b) (c)

Fig. 3 - S. Caorsi *et al.*, "Location and Imaging of ..."

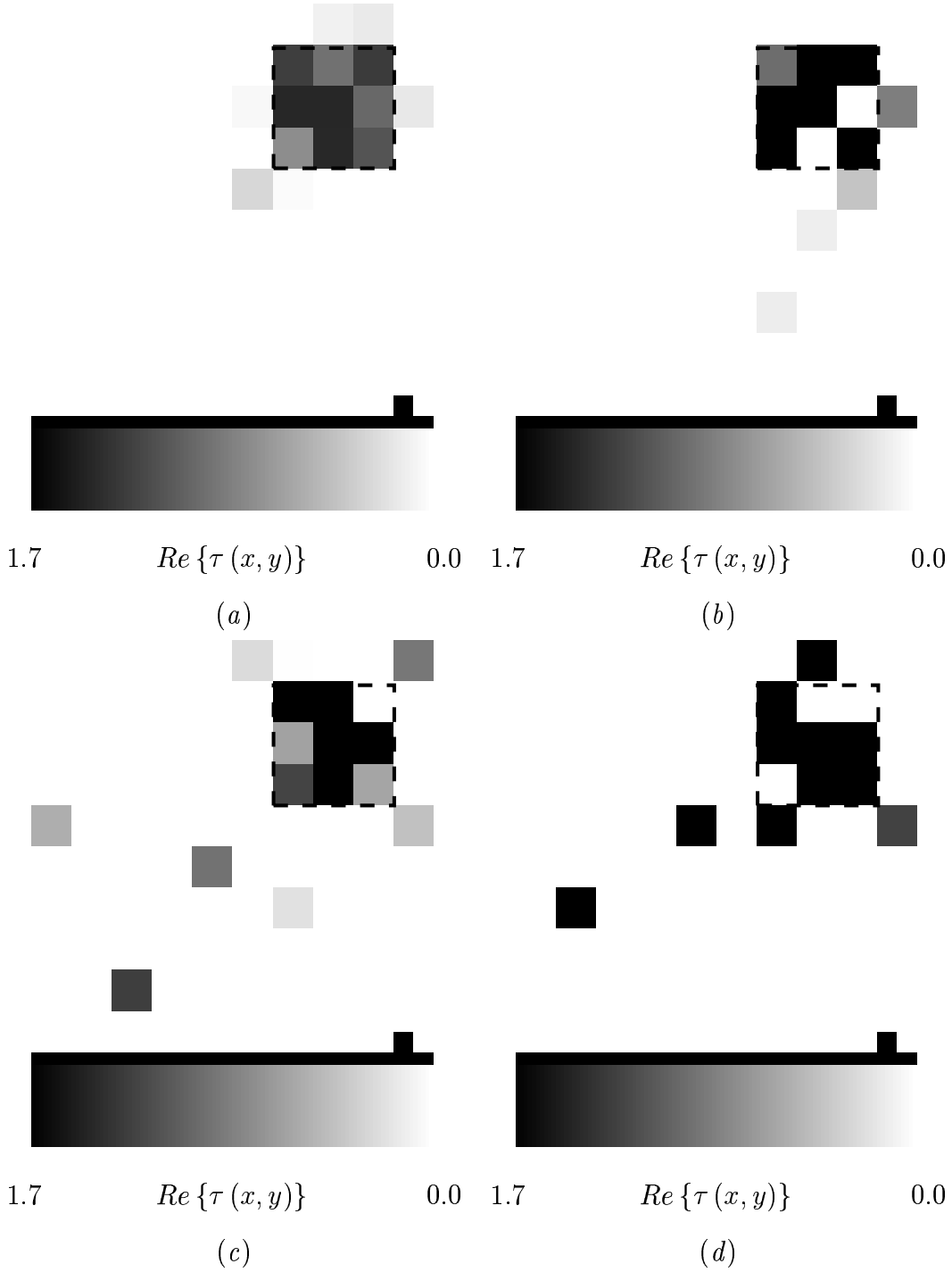

Fig. 4 - S. Caorsi *et al.*, "Location and Imaging of ..."

	χ_{tot}	χ_{int}	χ_{ext}
GC	5.7	15.0	4.80
GA	1.8	9.0	1.02
PSO	1.7	8.9	1.03

Tab. I - S. Caorsi *et al.*, "Location and Imaging of ..."

$SNR\ [dB]$	k^{opt}	Φ^{opt}	χ_{tot}	χ_{int}	χ_{ext}
30	0.7×10^4	1.0×10^{-4}	1.71	9.29	0.96
20	1.5×10^4	9.4×10^{-3}	3.38	20.97	1.64
10	2.0×10^4	3.9×10^{-2}	6.37	20.19	5.01
5	2.0×10^4	1.1×10^{-1}	10.34	25.33	8.86

Tab. II - S. Caorsi *et al.*, "Location and Imaging of ..."